AIP | Journal of Applied Physics

Antiparallel interface coupling evidenced by negative rotatable anisotropy in IrMn/NiFe bilayers

D. Schafer, P. L. Grande, L. G. Pereira, G. M. Azevedo, A. Harres, M. A. de Sousa, F. Pelegrini, and J. Geshev

Citation: Journal of Applied Physics **117**, 215301 (2015); doi: 10.1063/1.4921863
View online: http://dx.doi.org/10.1063/1.4921863
View Table of Contents: http://scitation.aip.org/content/aip/journal/jap/117/21?ver=pdfcov
Published by the AIP Publishing

Antiparallel interface coupling evidenced by negative rotatable anisotropy in IrMn/NiFe bilayers

D. Schafer,[1] P. L. Grande,[1] L. G. Pereira,[1] G. M. Azevedo,[1] A. Harres,[1] M. A. de Sousa,[2,3] F. Pelegrini,[2] and J. Geshev[1]
[1]*Instituto de Física, UFRGS, Porto Alegre, 91501-970 Rio Grande do Sul, Brazil*
[2]*Instituto de Física, UFG, Goiânia, 74001-970 Goiás, Brazil*
[3]*Centro Brasileiro de Pesquisas Físicas, Rio de Janeiro, 22290-180 Rio de Janeiro, Brazil*

(Received 27 February 2015; accepted 18 May 2015; published online 1 June 2015)

Negative rotatable anisotropy is estimated via ferromagnetic resonance measurements in as-made, annealed, and ion-irradiated $IrMn_3/Ni_{81}Fe_{19}$ bilayers. Opposite to previous observations, inverse correlation between rotatable anisotropy and coercivity is observed. The exchange-bias field, determined from hysteresis loop measurements, is higher than that obtained from ferromagnetic resonance for all samples. The results are discussed in terms of majority antiparallel coupling and magnetic-field-induced transitions from antiparallel to parallel states of uncompensated spins at ferromagnet/antiferromagnet interface. We affirm that an observation of negative rotatable anisotropy evidences antiparallel coupling even in systems presenting conventional exchange bias. © *2015 AIP Publishing LLC*. [http://dx.doi.org/10.1063/1.4921863]

I. INTRODUCTION

The exchange bias (EB) phenomenon,[1] which occurs when a magnetically hard material — usually an antiferromagnet (AF) — is coupled to an adjacent soft ferromagnet (FM), has been extensively studied, and is widely used in spin-valve and magnetic-tunnel-junction devices. Typically, the EB is negative, i.e., the hysteresis loop shift (H_{eb}) is opposite to the direction of the magnetic field (**H**) applied during either sample growth or post-deposition annealing or low-energy light-ion bombardment (IB). The positive exchange bias (PEB), i.e., a shift in the applied field direction, has become largely known after its observation in Fe/FeF_2.[2] Though required condition for PEB is usually thought to be an antiparallel coupling at the FM/AF interface,[2–7] observation of PEB near the blocking temperature has been attributed to reversible changes in the interfacial pinning,[8,9] long-range oscillatory Ruderman-Kittel-Kasuya-Yosida interaction that leads to a spin-glass state,[10] crystallography-driven rotation of the effective anisotropy and EB axes,[11] or frustration effects due to competition between the FM and AF exchange interactions.[12]

EB frequently implies an enhancement of the coercive field (H_C) compared to that of the FM alone.[1,13] Polycrystalline AF models[14,15] usually assume that magnetic moments with high anisotropy pin the FM magnetization (**M**) while low-anisotropy ones rotate with **M** during its reversal thus increasing H_C. However, it has been predicted[16] and recently confirmed[17] that a highly anisotropic uncompensated spin (UCS) would contribute to H_C and not to the bias if the coupling with **M** is strong enough, while a low-anisotropy spin enhances H_{EB} if the respective exchange coupling is sufficiently weak. The rotatable UCSs are also assumed to be responsible for the isotropic shift of the angular variation of the resonance field (H_{res}) in ferromagnetic resonance (FMR) measurements through a rotatable anisotropy (RA) field ($\mathbf{H_{RA}}$) that rotates with **M**.[15] Until recently, it has been considered that at magnetic saturation $\mathbf{H_{res}} = \mathbf{H} + \mathbf{H_{RA}}$, being $\mathbf{H_{RA}}$ parallel to **H** resulting in a positive RA, i.e., the inclusion of RA shifts $H_{res}(\phi_H)$ downward.[15] Here, ϕ_H is the in-plane field angle and $\phi_H = 0$ denotes the EB direction, i.e., that of **H** used to initialize the bias. It is worth noting that RA and anisotropy of rotatable UCSs are distinct properties: RA is an additional anisotropy of the FM that accounts for the interaction with rotatable UCSs, each of the latter characterized by anisotropy constant k_{rot}.

In this work, we address the origin of another fascinating EB feature, namely, the recently discovered *negative* RA. Opposite to the previous observations, in IrMn/Cr/Co films $\mathbf{H_{RA}}$ is antiparallel to **H** and the isotropic shift of $H_{res}(\phi_H)$ is upward,[18] i.e., $H_{RA} < 0$, which has been attributed to antiferromagnetic Co/Cr exchange coupling. The increase of $|H_{RA}|$ has also led to a significant increase of H_C. Negative RA has also been obtained in FeMn/Co[19] and NiFe/IrMn[20] films. Here, we report IB-induced variation of negative RA in IrMn/NiFe bilayers where, however, the correlation between RA and H_C is inverse. These results are discussed in terms of magnetic-field-induced transitions from antiparallel to parallel states.

II. EXPERIMENTAL

A $Si(100)/Ni_{53}Cr_{47}$(6 nm)/AF/FM/Cr(4 nm) polycrystalline film was grown from Ni, Cr, $Ni_{81}Fe_{19}$, and $Ir_{20}Mn_{80}$ targets via magnetron sputtering using an AJA Orion-8 UHV system at room temperature (RT) in the presence of a 130 Oe in-plane magnetic field. Here, FM denotes a 5 nm thick NiFe layer and AF refers to an IrMn layer with thickness of 7 nm. The nonmagnetic NiCr buffer layer[21,22] was deposited in order to induce the required for bias IrMn(111) texture[23] whereas the Cr cap layer was deposited in order to avoid oxidation. The pressure prior deposition was 1×10^{-8} Torr; during deposition it was kept at 7.5 mTorr for the IrMn layer and at 2 mTorr for the other ones using a 20 sccm Ar flow. After being structurally characterized, pieces of the film

were submitted to either magnetic annealing (MA) or IB. The MA sample was kept at 483 K during 15 min under a base pressure of 3×10^{-5} Torr in the presence of a 2.5 kOe magnetic field applied in the plane of the film. The IB was done at RT with 40 keV He ions at fluences ranging from 5×10^{13} to 1×10^{16} ions/cm^2 for constant flux of 100 nA/cm^2, also in the presence of an in-plane magnetic field of 5.5 kOe.

The stoichiometry of the layers was determined via Rutherford Backscattering Spectrometry (RBS) measurements from thick films of each material using 2 MeV He ions with perpendicular incidence of the ions relative to the film plane and backscattering angle of 165 degrees. The structural characterization of the as-made sample was done with the help of transmission electron microscopy (TEM), used to obtain bright-field images in cross-section geometry using a 200 kV JEOL JEM 2010 microscope. Medium energy ion scattering (MEIS) measurements were performed with 150 keV He ions with ion-beam incidence perpendicular to the sample plane.

Figure 1 gives a TEM bright-field image from the as-made sample, showing that the interfaces of the IrMn layer are even and sharp, denoting an insignificant roughness and interdiffusion. The identification of the other layers cannot be done due to the proximity in atomic mass of the constituting elements. Structural comparison between as-made, MA, and IB samples was not done using TEM, because the sample preparation process is destructive and it can induce structural changes and differences in the results.

MEIS measurements, see Fig. 2, show the Ir signal well-separated from those of the other elements because of its larger mass. The contributions of the other constituent elements are not resolved due to their mass proximity. The three spectra are practically indistinguishable, indicating that no sizeable (at least 5 Å interdiffusion of Ir atoms) modifications are induced by any of the post-deposition treatments. This is in agreement with literature data for EB systems that

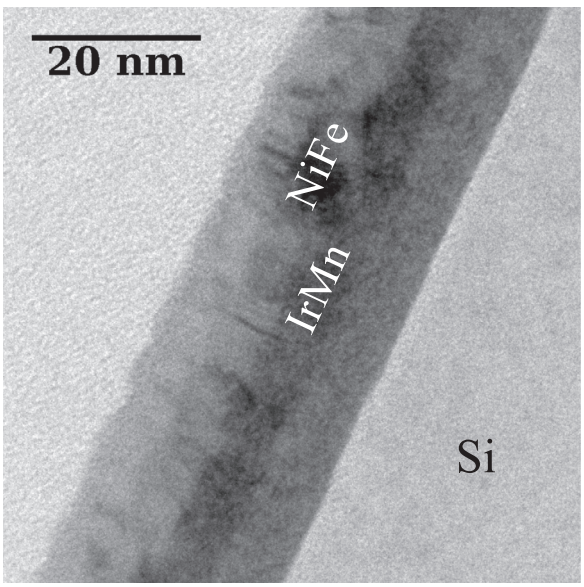

FIG. 1. TEM image from the as-made film.

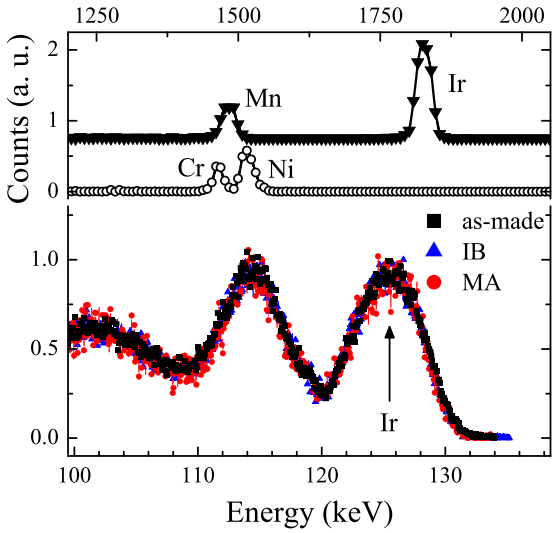

FIG. 2. Top: RBS data of the $Ni_{53}Cr_{47}$(6 nm) and $IrMn_3$(25 mn) films. Bottom: MEIS spectra of the as-made and MA films together with the ion-bombarded (at a fluence of 5×10^{15} ions/cm^2) sample.

show no structural modifications after either He or heavier ions (like Ga) bombardments,[24] although for other systems like Co/Pt, an intermixing has been seen even when He ions at low fluence are used.[25] RBS data obtained on NiCr(6 nm) and IrMn(25 nm) films, grown at the same conditions as those showing EB, are shown in Fig. 2. Their stoichiometry can be determined from the ratio of the peak areas weighted with the corresponding backscattering cross sections of each element;[26] our alloys were determined to be $IrMn_3$ and $Ni_{53}Cr_{47}$.

X-ray fine structure spectroscopy measurements were performed at the Brazilian Synchrotron Light Source (LNLS), where Mn *K*-edge spectra were collected in fluorescence detection mode. However, since full-multiple-scattering calculations did not reproduce the X-Ray-absorption near-edge structure (XANES) experiments, no decisive conclusions from these experiments were drown.

The values of the EB shift (H_{eb}^{MAG}) and H_C are extracted from RT magnetization hysteresis loops measured via alternating gradient force magnetometry. Special care was taken to assure that the data are collected after time interval sufficient to avoid temporal changes of H_{eb} (thermal drift effect[27]). Also, the maximum measurement field was sufficiently high to avoid EB overestimation due to minor-loops effects.[28] FMR experiments were performed using the *X*-band excitation frequency of 9.79 GHz, also at RT.

III. RESULTS AND DISCUSSION

Easy-axis hysteresis loops for the as-made and MA samples together with those of the sample submitted to IB at a fluence of 5×10^{15} ions/cm^2 are plotted in Fig. 3. The as-made sample already presents bias induced during the deposition since the first-grown AF layers are still weakly interacting so the coupling to the subjacent FM layer creates a significant number of uncompensated spins at the AF part of the interface.[29]

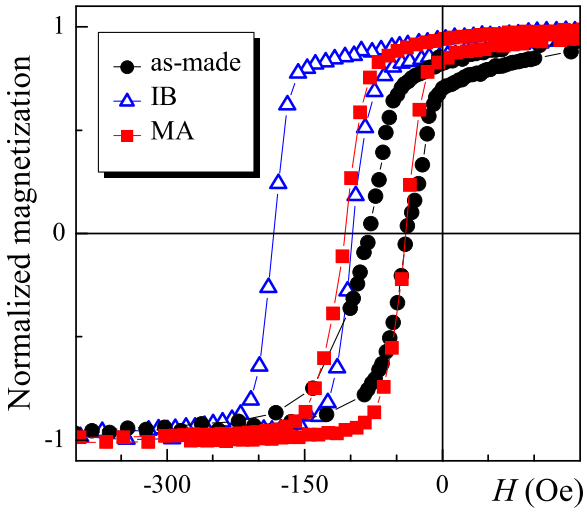

FIG. 3. Easy-axis hysteresis loops for the as-made, annealed, and ion-bombarded (at a fluence of 5×10^{15} ions/cm^2) samples. The lines are only guides to the eyes.

Figure 4 shows $H_{res}(\phi_H)$ experimental data for two representative IB samples together with the best fitting curves calculated as described below. Model simulations are frequently used in order to extract the anisotropy and coupling parameters from experimental data of complex magnetic systems, e.g., films consisting of at least two possibly interacting magnetic phases. In the case of FMR data interpretation, such a procedure seems indispensable. The magnetic parameters of our bilayers were estimated by employing a slightly modified version of a previously described model[30] considering a polycrystalline FM film divided into a number of grains, each of them with saturation magnetization M_s, volume V, thickness t, anisotropy constant K_U, and easy-axis direction given by the unit vector $\hat{\mathbf{u}}$. These FM grains interact with UCSs located at the AF/FM interface. Each UCS could be classified as unstable, either superparamagnetic or rotatable (with magnetization $\mathbf{m_{rot}}$ and volume v_{rot}) or stable.

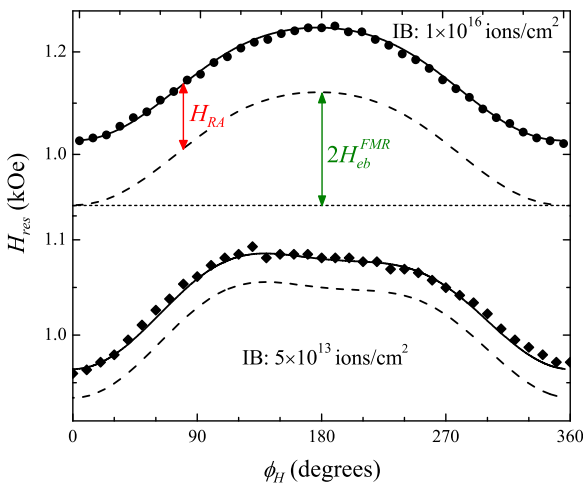

FIG. 4. Angular variations of H_{res} extracted from X-band FMR measurements for samples bombarded using two different ion fluences, i.e., 1×10^{16} ions/cm^2 (top panel) and 5×10^{13} ions/cm^2 (bottom panel). The solid lines are simulated with the model presented in the text; the dashed lines represent the same simulations assuming $H_{RA} = 0$.

The latter could be either set (biasing, with magnetization $\mathbf{m_{set}}$, volume v_{set}, anisotropy constant k_{set}, and easy-axis direction given by the unit vector $\hat{\mathbf{s}}$), aligned with $\mathbf{H}$ during the preparation or post-treatment procedure of the sample, or unset, i.e., an UCS that cannot be reversed during the treatment. Superparamagnetic and unset UCSs do not contribute to either H_{eb} or H_C. The free energy of a FM grain, coupled to biasing and/or rotatable UCSs, is

$$E = E_{FM} + E_{ucs} + E_{int}, \tag{1}$$

where E_{FM} includes the FM's demagnetization, uniaxial, and RA anisotropy terms together with the Zeeman one

$$E_{FM}/V = 2\pi(\mathbf{M_s} \cdot \hat{\mathbf{n}})^2 - K_U \frac{(\mathbf{M_s} \cdot \hat{\mathbf{u}})^2}{M_s^2} - \mathbf{H_{RA}} \cdot \mathbf{M_s} - \mathbf{H} \cdot \mathbf{M_s}. \tag{2}$$

Here, the unit vector $\hat{\mathbf{n}}$ gives the direction of the normal to the film's plane. E_{ucs} includes the anisotropy and Zeeman terms of a $\mathbf{m_{set}}$

$$E_{ucs}/v_{set} = -k_{set} \frac{(\mathbf{m_{set}} \cdot \hat{\mathbf{s}})^2}{m_{set}^2} - \mathbf{H} \cdot \mathbf{m_{set}}. \tag{3}$$

The last term in Eq. (1) corresponds to the interface exchange coupling between the FM and the biasing UCS, $E_{int} = -J\,\mathbf{M_s} \cdot \mathbf{m_{set}}/(M_s\, m_{set})$, being J the respective coupling constant. In the present study, $\mathbf{H}$ has been applied in the film plane. The equilibrium angles of $\mathbf{M_s}$ and $\mathbf{m_{set}}$ were determined by minimizing the energy expression given by Eq. (1); more details can be found elsewhere.[18,30,31] Differently from the previously employed domain-wall formation model,[32] we use uniaxial UCSs as FM's pinning sites instead of interfacial AF domain wall. Note that $\mathbf{m_{set}} \parallel \hat{\mathbf{s}}$ for very high k_{set} and the model is reduced[33] to the rigid AF moment (RAF) model. The good agreement between model and experiment confirms that the biasing UCSs of our films present very strong anisotropy fields as compared to the coupling field H_E [$= J/(M_s t)$].

The FMR-estimated EB field has been defined[15,30] as $H_{eb}^{FMR}(\phi_H) = \frac{1}{2}|H_{res}(\phi_H) - H_{res}(\phi_H + \pi)|$. In the framework of the RAF model, $H_E \approx H_{eb}^{FMR}$ taken at[30,34] $\phi_H = 0$, so the values of H_{eb}^{FMR} from Fig. 5 were used as H_E ones in the simulations together with $K_U = 1.95 \times 10^4$ erg/cm^3 and the literature values of 780 emu/cm^3 for M_s and 2.09 for the effective gyromagnetic factor. Thus, the only parameter varied in order to fit H_{res} data was H_{RA}.

The bias, coercivity, and RA dependencies on the IB fluence are given in Fig. 5. The H_{eb} variation is typical for most AF/FM systems, attributed to defects created by IB. Nuclear energy losses of the impinging ions[35,36] in the bulk of the AF lead to a reduction of the AF anisotropy constant (K_{AF}) resulting in an increase of the number of interfacial UCSs due to the exchange coupling to the saturated FM; on the other hand, defects created at the AF/FM interface lead to a decrease of the coupling and, consequently, to a reduction of H_{eb}.[37] For high fluences, the decrease of K_{AF} would be more drastic and the interfacial defects become important. It has

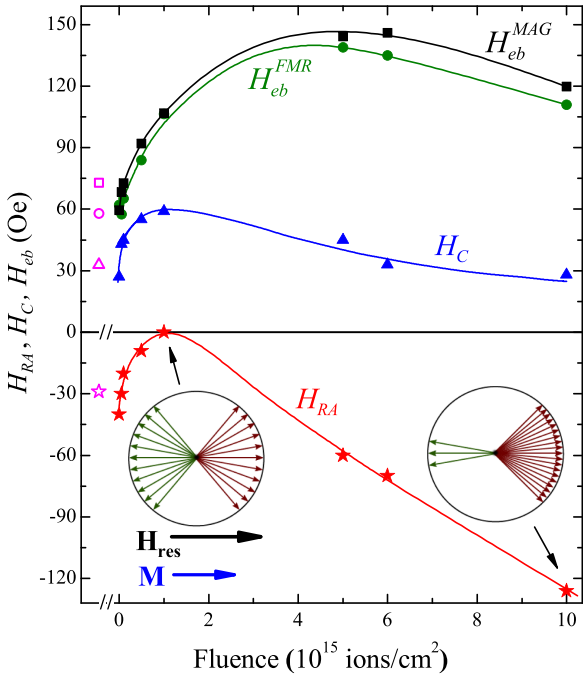

FIG. 5. H_{eb}^{MAG}, H_{eb}^{FMR}, $H_{C,}$ and H_{RA} as a function of the ion fluence. The empty symbols correspond to the annealed sample and the lines are only guides to the eyes. Schematic distributions of the rotatable grains' magnetizations at $H = H_{res}$, assuming that these are antiparallel coupled to the FM, are illustrated for two representative fluences.

been reported that irradiation with Ar^+ ions in a presence of magnetic field may change the direction and dispersion of the anisotropy of NiFe films.[38] In FMR experiments, such effects could be detected as a modification of the FM's anisotropy and/or a misalignment between the FM and AF easy axes. Our FMR fitting results, however, strongly indicate that K_U does not change significantly after IB; for some samples, a misalignment of only a few degrees between the FM and AF easy axes was observed. The latter, however, should not be attributed to IB since the magnetic field used to initialize the bias was the same for both FM and AF already deposited layers. Thus, we will not consider changes on the FM as an important mechanism responsible for the reported results.

For all fluences, our films present (i) negative or zero H_{RA} values, (ii) inverse correlation between $|H_{RA}|$ and H_C, and (iii) $H_{eb}^{MAG} > H_{eb}^{FMR}$.

We assert that majority antiparallel coupling and field-induced spin-flip transitions of the interfacial spins is the key for the occurrence of negative RA and for the elucidation of the other two peculiar features cited above. The conjecture of antiparallel coupling at the IrMn/NiFe interface agrees with works on the same system.[6,39] Experiments[40] and calculations[41] have established the antiparallel Fe-Mn configuration for small surface coverage of Mn atoms. It has also been claimed that at IrMn/CoFeB interfaces uncompensated Mn spins can couple antiferromagnetically to the FM spins resulting in PEB.[7,42] Our data are consistent with a scenario where parallel and antiparallel couplings between the FM and UCSs coexist[6] due to, e.g., the multiple chemical elements present in this region. Two possible interface bonding types are Fe-Mn and Ni-Mn.

Figure 6 gives a schematic of the orientations of **M** and the two types of interface UCSs in the low (a hysteresis-loop trace) and high (H_{res}) field regions. For better visualization, the simple case of **H** applied along the common easy axis of the FM and both types of grains with UCSs is exemplified. Recall that the EB remains negative even when **M** and $\mathbf{m_{set}}$ are antiparallel coupled ($J < 0$) provided that $\mathbf{m_{set}}$ maintains its direction opposite to that of the EB setting field. If a very strong magnetic field is able to induce the reorientation of $\mathbf{m_{set}}$ from antiparallel to parallel state and by some reason this orientation is frozen, this UCS will contribute to PEB in a subsequent measurement.[2] If, however, when lowering back the field the antiparallel alignment is restored, this $\mathbf{m_{set}}$ will add to negative EB in the consequent measurement as long as the maximum field used saturates the FM.

It is recognized that different measurement techniques could yield distinct EB values. For example, the discrepancy between H_{eb}^{MAG} and H_{eb}^{FMR} has been attributed[30] to the physical mechanisms involved in each technique. Usually $H_{eb}^{MAG} < H_{eb}^{FMR}$ given that UCSs, which are stable in perturbative experiments like FMR, could be unstable in a magnetization curve trace seeing as the measurement time of the latter is longer than the relaxation time.[18,31,34,43]

Our samples, however, show $H_{eb}^{MAG} > H_{eb}^{FMR}$. The mechanism of field-induced flips naturally elucidates this finding on condition that H_{res} is high enough to initially induce the antiparallel-parallel reorientation, which is afterward restored when lowering the field. That is, while in the FMR experiments an antiparallel-coupled though flipped $\mathbf{m_{set}}$ lessens the ordinary EB and contributes to the negative RA, see below, it adds to the negative H_{eb}^{MAG} resulting in the observed here $H_{eb}^{MAG} > H_{eb}^{FMR}$.

Regardless of the type, parallel or antiparallel, of the M/m_{rot} coupling and its strength (J'), H_C of an FM/AF bilayer should be enhanced if compared to that of the respective control FM film due to the additional energy necessary to reverse an anisotropic UCS. The same holds for the RA, always positive for $J' > 0$. Moreover, it remains positive even for $J' < 0$ as long as the measurement field (here, H_{res}) is not strong enough to induce the antiparallel-parallel transition of rotatable UCSs. Negative RA can only be obtained if such transitions occur arising from the competition between the Zeeman term, the UCSs' anisotropy field $H_{A,rot}$ ($=2k_{rot}/m_{rot}$), and J'. Note that accounting for the frequently neglected Zeeman term is essential for understanding the negative RA. The free energy (E) of a (coupled to the FM) grain with rotatable UCS in a magnetic field consists of its anisotropy, coupling and Zeeman terms. For saturated FM, i.e., $\mathbf{M} \parallel \mathbf{H}$, it is straightforward to show that

$$\frac{E}{v_{rot}\, m_{rot}} = \frac{1}{2} H_{A,rot} \sin^2 \phi_{rot} - H' \cos(\phi_H - \phi_{rot}),$$

where $H' = H + J'/m_{rot}$. For negative J' and **H** parallel to the easy axis of $\mathbf{m_{rot}}$, the latter will flip to be parallel to **H** and, consequently, to **M**, if $H > H_{A,rot} - J'/m_{rot}$; it will flip back at a field equal to $H_{A,rot} + J'/m_{rot}$. These transitions are sketched in Fig. 6. When flipped, UCSs with negative J'

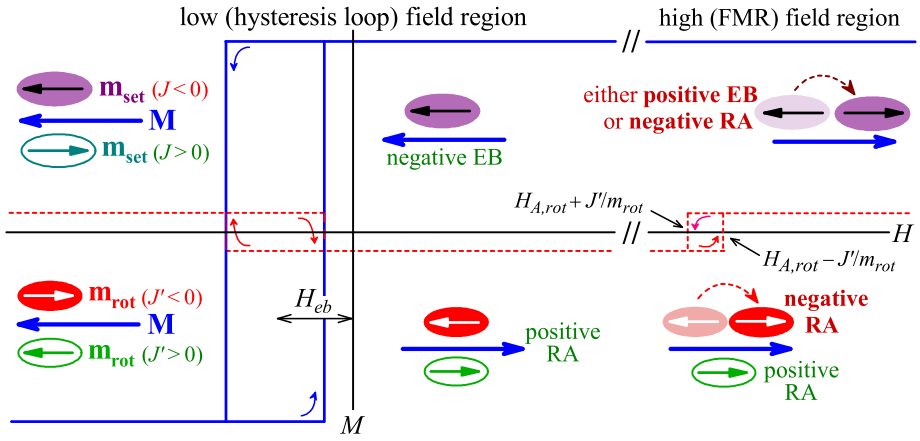

FIG. 6. Schematic of the orientations of **M**, $\mathbf{m}_{set}$, and $\mathbf{m}_{rot}$ in the field region of a hysteresis-loop trace and in that of strong magnetic fields (i.e., that of H_{res}). **H** is applied along the easy direction of $\mathbf{m}_{set}$ (and of $\mathbf{m}_{rot}$). Both parallel and antiparallel FM/UCS alignments are considered. The hysteresis loop of **M** (solid curve) and that of $\mathbf{m}_{rot}$ AF-coupled to **M** (dashed curve) are plotted, where the solid curved arrows indicate the magnetization paths. The dashed curved arrows represent magnetic-field-induced spin-flip-like transitions responsible for either negative FMR-estimated RA or positive EB.

contribute to the negative RA. As normally UCSs present distributions in k_{rot} and J', the lower $H_{A,rot}$ and/or the greater $|J'|$, the smaller the field required for a flip, the greater the number of flipped UCSs (see the schematics in Fig. 5) and, consequently, the greater $|H_{RA}|$. Since there might exist rotatable UCSs with $J'>0$ contributing "positively" to the RA, the point of $H_{RA}=0$ in Fig. 5 does not necessarily correspond to equal numbers of flipped and unflipped UCSs.

Due to the direct correlation between H_C and k_{rot}, see above, the latter should vary with the ion fluence in a way qualitatively similar to that of H_C, see Fig. 5; the mechanisms involved are, most probably, those responsible for the already discussed EB variations. However, as demonstrated above, the variations of $|H_{RA}|$ and k_{rot} of the susceptible to field-induced antiparallel-parallel transitions UCSs are opposite, thus explaining the observed here anticorrelation between H_C and RA. Nevertheless, this does not contradict the concept that the rotatable UCSs are responsible for the coercivity enhancement.

An increase in number of prone to flip UCSs would also add to the negative RA: the greater the number of rotatable UCSs in a hysteresis loop trace the higher H_C. This seems to be the case of IrMn/Cr/Co,[18] resulting in the direct correlation between H_C and $|H_{RA}|$.

It is worth noting that a model which takes into account such field-induced spin-flip transitions of the interfacial spins[16] has been able to reproduce the PEB induced by athermal training[6] as well as the recovery of training after application of strong magnetic fields.[44]

IV. CONCLUSIONS

We have shown that the recently discovered negative rotatable anisotropy is a signature of antiparallel interface coupling and magnetic-field-induced spin-flip-like transitions of uncompensated spins. This mechanism explains the observed here inverse correlation between rotatable anisotropy and coercivity as well as the lower bias values yield from FMR experiments as compared to those estimated from hysteresis loop measurements in IrMn/NiFe bilayers. It is also able to account for previously observed training-induced positive exchange bias and partial recovery of training after application of strong magnetic fields. We thus conclude that experimental observations of negative rotatable anisotropy provide evidences for antiparallel interface coupling even in systems presenting conventional exchange bias only.

ACKNOWLEDGMENTS

J.G. appreciates useful discussions with J. Nogués. We acknowledge LNLS for the synchrotron beamtime at the D08B-XAFS2 beamline. Part of this work was developed in collaboration with the Ion Implantation Laboratory at IF-UFRGS. The sputtering deposition was performed at LCN, IF-UFRGS. Work supported by CNPq (Project Nos. 475499/2009-3, 307082/2012-1, and 483277/2012-6) and PRONEX.

[1]W. H. Meiklejohn and C. P. Bean, Phys. Rev. **102**, 1413 (1956); **105**, 904 (1957).
[2]J. Nogués, D. Lederman, T. J. Moran, and I. K. Schuller, Phys. Rev. Lett. **76**, 4624 (1996).
[3]J. Nogués, C. Leighton, and I. K. Schuller, Phys. Rev. B **61**, 1315 (2000).
[4]H. Ohldag, H. Shi, E. Arenholz, J. Stöhr, and D. Lederman, Phys. Rev. Lett. **96**, 027203 (2006).
[5]C. Leighton, J. Nogués, B. J. Jönsson-Åkerman, and I. K. Schuller, Phys. Rev. Lett. **84**, 3466 (2000).
[6]S. K. Mishra, F. Radu, H. A. Dürr, and W. Eberhardt, Phys. Rev. Lett. **102**, 177208 (2009).
[7]H. Fulara, S. Chaudhary, S. C. Kashyap, and D. K. Pandya, J. Appl. Phys. **110**, 093916 (2011).
[8]T. Gredig, I. N. Krivorotov, P. Eames, and E. D. Dahlberg, Appl. Phys. Lett. **81**, 1270 (2002).
[9]C. Prados, E. Pina, A. Hernando, and A. Montone, J. Phys.: Condens. Matter **14**, 10063 (2002).
[10]M. Ali, P. Adie, C. H. Marrows, D. Greig, B. J. Hickey, and R. L. Stamps, Nat. Mater. **6**, 70 (2007).
[11]A. K. Suszka, O. Idigoras, E. Nikulina, A. Chuvilin, and A. Berger, Phys. Rev. Lett. **109**, 177205 (2012).
[12]Z. R. Li, W. B. Mi, X. C. Wang, and H. L. Bai, J. Magn. Magn. Mater. **379**, 124 (2015).
[13]J. Nogués and I. K. Schuller, J. Magn. Magn. Mater. **192**, 203 (1999).
[14]E. Fulcomer and S. Charap, J. Appl. Phys. **43**, 4190 (1972).
[15]R. D. McMichael, M. D. Stiles, P. J. Chen, and W. F. Egelhoff, Jr., Phys. Rev. B **58**, 8605 (1998).
[16]A. Harres and J. Geshev, J. Phys.: Condens. Matter **23**, 216003 (2011); **24**, 326004 (2012).

[17]T. Dias, E. Menéndez, H. Liu, C. Van Haesendonck, A. Vantomme, K. Temst, J. E. Schmidt, R. Giulian, and J. Geshev, J. Appl. Phys. **115**, 243903 (2014).
[18]S. Nicolodi, L. G. Pereira, A. Harres, G. M. Azevedo, J. E. Schmidt, I. García-Aguilar, N. M. Souza-Neto, C. Deranlot, F. Petroff, and J. Geshev, Phys. Rev. B **85**, 224438 (2012).
[19]P. G. Barreto, M. A. Sousa, F. Pelegrini, W. Alayo, F. J. Litterst, and E. Baggio-Saitovitch, Appl. Phys. Lett. **104**, 202403 (2014).
[20]M. A. de Sousa, F. Pelegrini, W. Alayo, J. Quispe-Marcatoma, and E. Baggio-Saitovitch, Phys. B: Condens. Matter **450**, 167 (2014).
[21]E. R. Jette, V. H. Nordstrom, B. Queneau, and F. Foote, Trans. Am. Inst. Mining Met. Engrs. **111**, 361 (1934).
[22]A. E. Berkowitz, G. F. Rodriguez, J. I. Hong, K. An, T. Hyeon, N. Agarwal, D. J. Smith, and E. E. Fullerton, Phys. Rev. B **77**, 024403 (2008).
[23]N. P. Aley, R. Kroeger, B. Lafferty, J. Agnew, Y. Lu, and K. O'Grady, IEEE Trans. Magn. **45**, 3869 (2009).
[24]S. Blomeier, D. McGrouther, S. McVitie, J. N. Chapman, M. C. Weber, B. Hillebrands, and J. Fassbender, Eur. Phys. J. B. **45**, 213 (2005).
[25]T. Devolder, Phys. Rev. B **62**, 5794 (2000).
[26]W.-K. Chu, J. W. Mayer, and M.-A. Nicolet, *Backscattering Spectrometry* (Academic Press, New York, 1978).
[27]A. Ehresmann, D. Junk, D. Engel, A. Paetzold, and K. Röll, J. Phys. D **38**, 801 (2005).
[28]L. Klein, Appl. Phys. Lett. **89**, 036101 (2006); J. Geshev, J. Magn. Magn. Mater. **320**, 600 (2008); Appl. Phys. Lett. **93**, 176101 (2008); J. Geshev, L. G. Pereira, and V. Skumryev, Phys. Rev. Lett. **100**, 039701 (2008); A. Harres, J. Geshev, and V. Skumryev, *ibid.* **114**, 099703 (2015).
[29]J. Geshev, T. Dias, S. Nicolodi, R. Cichelero, A. Harres, J. J. S. Acuña, L. G. Pereira, J. E. Schmidt, C. Deranlot, and F. Petroff, J. Phys. D: Appl. Phys. **44**, 095002 (2011).
[30]J. Geshev, L. G. Pereira, and J. E. Schmidt, Phys. Rev. B **64**, 184411 (2001).
[31]J. Geshev, S. Nicolodi, L. G. Pereira, L. C. C. M. Nagamine, J. E. Schmidt, C. Deranlot, F. Petroff, R. L. Rodríguez-Suárez, and A. Azevedo, Phys. Rev. B **75**, 214402 (2007).
[32]D. Mauri, H. C. Siegmann, P. S. Bagus, and E. Kay, J. Appl. Phys. **62**, 3047 (1987).
[33]J. Camarero, J. Sort, A. Hoffmann, J. M. García-Martín, B. Dieny, R. Miranda, and J. Nogués, Phys. Rev. Lett. **95**, 057204 (2005).
[34]H. Xi, R. M. White, and S. M. Rezende, Phys. Rev. B **60**, 14837 (1999).
[35]D. Engel, A. Ehresmann, J. Schmalhorst, M. Sacher, V. Höink, and G. Reiss, J. Magn. Magn. Mater. **293**, 849 (2005).
[36]D. Schafer, J. Geshev, S. Nicolodi, L. G. Pereira, J. E. Schmidt, and P. L. Grande, Appl. Phys. Lett. **93**, 042501 (2008).
[37]A. Ehresmann, Recent Res. Dev. Appl. Phys. **7**, 1 (2004).
[38]S. I. Woods, S. Ingvarsson, J. R. Kirtley, H. F. Hamann, and R. H. Koch, Appl. Phys. Lett. **81**, 1267 (2002).
[39]G. Salazar-Alvarez, J. J. Kavich, J. Sort, A. Mugarza, S. Stepanow, A. Potenza, H. Marchetto, S. S. Dhesi, V. Baltz, B. Dieny, A. Weber, L. J. Heyderman, J. Nogués, and P. Gambardella, Appl. Phys. Lett. **95**, 012510 (2009).
[40]O. Rader, W. Gudat, D. Schmitz, C. Carbone, and W. Eberhardt, Phys. Rev. **B 56**, 5053 (1997).
[41]S. Bouarab, H. Nait-Laziz, M. A. Khan, C. Demangeat, H. Dreyssé, and M. Benakki, Phys. Rev. B **52**, 10127 (1995).
[42]T. Eimüller, T. Kato, T. Mizuno, S. Tsunashima, C. Quitmann, T. Ramsvik, S. Iwata, and G. Schütz, Appl. Phys. Lett. **85**, 2310 (2004).
[43]B. H. Miller and E. Dan Dahlberg, Appl. Phys. Lett. **69**, 3932 (1996).
[44]S. Brems, D. Buntinx, K. Temst, C. Van Haesendonck, F. Radu, and H. Zabel, Phys. Rev. Lett. **95**, 157202 (2005).